ACS OMEGA

Open Access



http://pubs.acs.org/journal/acsodf

Article

# Crosslinked PVA-*g*-poly(AMPS) Nanogels for Enhanced Solubility and Dissolution of Ticagrelor: Synthesis, Characterization, and Toxicity Evaluation

Usman Saleem, Ikrima Khalid,* Liaqat Hussain, Abdulrahman Alshammari, and Norah A. Albekairi

Cite This: *ACS Omega* 2024, 9, 21401−21415

Read Online

ACCESS | Metrics & More | Article Recommendations

**ABSTRACT:** In this study, we synthesized PVA-*g*-poly(AMPS) nanogels with the aim of enhancing the solubility and dissolution of ticagrelor (TGR). Ticagrelor, a noncompetitive, reversible P2Y12 receptor antagonist, is prescribed to treat acute coronary syndrome. Ticagrelor has restricted oral bioavailability (≈36%) because of its poor solubility and permeability. The free radical polymerization methodology was employed to synthesize nanogels with varied concentrations of poly(vinyl alcohol) (polymer), 2-acrylamido-2-methylpropanesulfonic acid (monomer), and *N*,*N*-methylene bis(acrylamide) (crosslinker). The prepared nanogels were analyzed by swelling studies, % drug entrapment efficiency (DEE), solubility studies, *in vitro* drug release studies, zeta sizer, Fourier transform infrared (FTIR) spectroscopy, powder X-ray diffraction (PXRD), thermogravimetric analysis (TGA), differential scanning calorimetry (DSC), and scanning electron microscopy (SEM). The optimized formulation (PA5) revealed a particle size of 45.86 nm, with a polydispersity index (PDI) of 0.41 and a %DEE of 85.1%. FTIR spectroscopy, XRD, and SEM confirmed the formation of crosslinked nanogels with amorphous and porous structures, and TGA/DSC proved their thermal stability. *In vitro* dissolution studies showed 99.91% drug release, and the ticagrelor solubility from the synthesized formulations was significantly improved up to 8.2-fold. All formulations followed the Korsmeyer−Peppas model with the Fickian diffusion as the release mechanism. The toxicity studies carried out on rats and the MTT assay on the Caco-2 cell line validated the biocompatibility of the nanogel formulations. The outcomes of the current study led to the conclusion that the PVA-*g*-poly(AMPS) nanogels synthesized by us could be used as dedicated pharmaceutical delivery systems to achieve enhanced solubility and dissolution of ticagrelor.

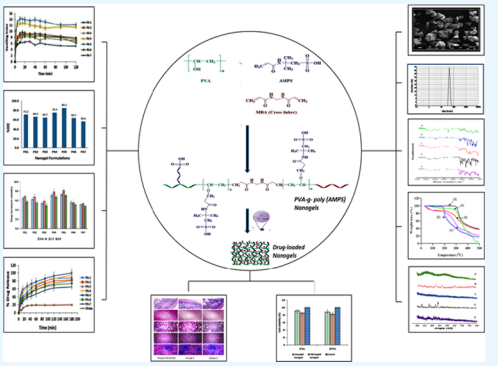

## 1. INTRODUCTION

A significant obstacle to the successful oral delivery of drugs is their inadequate solubility.[1] The literature reports that a large proportion of marketed (≈40%) and investigational (≈75%) drugs exhibit low aqueous solubility profiles.[2] The low solubility of a drug is consistent with low bioavailability and reduced therapeutic outcomes because these drugs are flushed away from the absorption site before their adequate dissolution. Numerous approaches have been investigated to tackle the problem of poor solubility such as amorphous solid dispersions, nanogels, solid lipid nanoparticles (SLNs), self-emulsifying systems (SMEDs and SNEDs), liposomes, cocrystallization, microneedles, nanoemulsions, nanosuspensions, cyclodextrin-based inclusion complexes, nanocapsules, dendrimers, cosolvency, and pH modification.[2,3]

Among the above cited techniques, nanogels have emerged as the most promising delivery vehicles due to nanosizing, hydrophilicity, high swellability, high drug entrapment efficiency, stability, biocompatibility, and economical manufacturing.[4] Nanogels are nanoscale versions of hydrogels, can accommodate both hydrophilic and hydrophobic drugs, and can be synthesized from natural or synthetic monomers and polymers or their combinations.[5] Various hydrophilic polymers and monomers such as poly(vinyl alcohol) (PVA), poly(vinylpyrrolidone) (PVP), chitosan, gelatin, poly(ethylene glycol) (PEG), *β*-cyclodextrin, poloxamer, sodium alginate, chondroitin sulfate, carbopol, hydroxy-propyl methylcellulose (HPMC), acrylamido methylpropanesulfonic acid (AMPS), acrylic acid, lactic acid (LA), and methacrylic acid (MAA) are commonly used for preparing nanogels.[6] Nanogels are networks that are physically (polymer chain entanglement, ionic interactions, and hydrogen bonding) or chemically (covalently) crosslinked and have the ability to imbibe, swell, and retain a large quantity of water and allow the tunable release of drugs without dissolving their intact structure.[7]

**Received:** February 22, 2024
**Revised:** March 29, 2024
**Accepted:** April 18, 2024
**Published:** May 2, 2024

Generally, chemically crosslinked nanogels have more mechanical strength and are more stable against environmental degradation than physically crosslinked nanogels.[8] Upon swelling, nanogels mimic body tissues due to their soft and rubbery nature and can reach the capillaries by penetrating the deeper tissues through different pathways.[9] Formulations based on nanogels may be administered by oral, topical, nasal, and ocular routes.[5,10] Nanogels have potential applications in the fields of pharmaceutical manufacturing, biomedicine, genetic engineering, agriculture, and food packaging.[11] Several previous studies have proven that nanogels are pivotal drug delivery systems for the solubility enhancement of active pharmaceutical ingredients.[4d9a12]

According to the World Health Organization (WHO) 2020 report, ischemic heart disease was the world's leading cause of death.[13] In 2022, cardiovascular diseases were associated with the highest number of deaths in the United States.[14] Acute coronary syndrome (ACS), an ischemic heart disease, describes a range of conditions associated with sudden reduced blood flow to the heart. Ticagrelor (TGR) is prescribed to reduce the incidence of myocardial infarction, stroke, and cardiovascular death in patients with ACS.[15] TGR, a cyclopentyl-triazolo-pyrimidine, is a novel class of antiplatelet drugs. It is a reversibly binding, noncompetitive antagonist of the P2Y12 receptor.[16] In comparison to clopidogrel, a frequently prescribed inhibitor of P2Y12, TGR significantly reduces the prevalence of cardiovascular death due to ACS, as reported by the Platelet Inhibition and Patient Outcomes (PLATO) study.[16] TGR does not require metabolic activation in contrast to its counterparts (*i.e.*, clopidogrel and prasugrel) and minimizes interindividual variations in therapeutic outcomes. Additionally, TGR exhibits a rapid offset of the antiplatelet effect compared to prasugrel, thus reducing the risk of side effects such as bleeding.[17] Because of the aforementioned reasons, TGR is currently preferred over other antiplatelets in clinical guidelines.[16,18] TGR has been reported to have low aqueous solubility (10−15 $\mu$g/mL) and low permeability, leading to a low oral bioavailability of ≈36%.[19] Therefore, the development of an adequate drug delivery system for enhancing the solubility of TGR and, ultimately, efficient ACS therapy is extremely important.

PVA is a synthetic polymer and potential material for a wide range of applications due to its hydrophilicity, biocompatibility, and biodegradability. PVA also exhibits other properties such as good film-forming ability, mechanical strength, and chemical resistance. Hydrogel formulations based on PVA have exhibited adequate mechanical strength and swelling index, advocating PVA as a promising ingredient.[20] AMPS grafting on the PVA backbone serves to impart attributes such as macropores, high porosity, and more swellability to the synthesized nanogels. AMPS, being a hydrophilic monomer, plays a crucial role in preparing nanogels due to sulfonic groups that are completely ionized to sulfonate ions irrespective of the pH of the medium. On increasing the AMPS concentration, the swelling index of nanogels increases, which is ascribed to the electrostatic repulsion generated among sulfonate ions, resulting in elevated porosity.[21]

A few formulation strategies, such as solid dispersion, self-microemulsification, nanostructured lipid carriers, and nanosuspension, have been adopted to augment the solubility and bioavailability of ticagrelor.[22] According to our knowledge, no formulation based on nanogels has been reported yet. Nanogels have garnered enormous interest in terms of solubility enhancement, biocompatibility, and ease of manufacturing.[4d12ad] Therefore, the current work is intended to synthesize and evaluate PVA-*g*-poly(AMPS) nanogels as promising delivery vehicles for enhancing the solubility and dissolution of ticagrelor. The free radical polymerization process was used to synthesize chemically crosslinked PVA-*g*-poly(AMPS) nanogels by utilizing the crosslinker methylene bis(acrylamide) (MBA). After fabricating the system, nanogels were subjected to physical and chemical characterization and toxicity studies to reveal their prospective advantages over other reported carrier systems by taking the drug release, solubility, crystallinity, biocompatibility, and economical manufacturing into consideration.

## 2. MATERIALS AND METHODS

**2.1. Chemicals.** Poly(vinyl alcohol) (PVA) (mol wt 9000−10,000), 2-acrylamido-2-methylpropanesulfonic acid (AMPS), and *N*,*N*-methylene bis(acrylamide) (MBA) were purchased from Sigma-Aldrich, Darmstadt, Germany. Ammonium persulfate (APS) was bought from AppliChem, Germany. All chemicals used were of analytical grade. Ticagrelor was received as a generous gift from CCL Pharmaceuticals (Pvt.) Ltd., Lahore, Pakistan.

**2.2. Methods.** *2.2.1. Synthesis of Nanogels.* The process of free radical polymerization was adopted to synthesize PVA-*g*-poly(AMPS) nanogels.[234d] Separate solutions were prepared for PVA, AMPS, MBA (crosslinker), and APS (initiator). A transparent solution of PVA was prepared in water at 50 °C with continuous stirring. Aqueous solutions of AMPS and APS were prepared separately by adding water and solubilizing under stirring at 200 rpm followed by mixing while continuously stirring at room temperature. The mixture of AMPS and APS was then transferred into a PVA solution (previously cooled) by stirring at 300 rpm at ambient temperature until a clear solution was obtained. To the as-prepared solution, a crosslinker (MBA) solution prepared in a water and ethanol (2:1) mixture was added dropwise at 50 °C while continuously stirring. For the removal of dissolved oxygen, nitrogen gas was continuously purged into the mixture for 15 min. The final mixture was then subjected to reflux condensation at 80 °C for 3−4 h for gelation. The prepared formulations were made free from uncrosslinked components by washing with a mixture of ethanol and water (1:1). Eventually, the collected formulations were subjected to sieving and subsequent drying in an oven at 40 °C to attain a constant weight. Table 1 shows varied compositions of different formulations. The proposed structure of the crosslinked nanogels is depicted in Figure 1.

*2.2.2. Drug Loading.* The drug was incorporated into the synthesized nanogels by the swelling diffusion method.[9a] For

**Table 1. Feed Scheme of PVA-*g*-poly (AMPS) Nanogels**

| sr., no. | formulation code | PVA (%w/w) | AMPS (%w/w) | APS (%w/w) | MBA (%w/w) |
|---|---|---|---|---|---|
| 1 | PA1 | 0.4 | 24 | 0.4 | 4 |
| 2 | PA2 | 0.8 | 24 | 0.4 | 4 |
| 3 | PA3 | 1.2 | 24 | 0.4 | 4 |
| 4 | PA4 | 0.4 | 32 | 0.4 | 4 |
| 5 | PA5 | 0.4 | 40 | 0.4 | 4 |
| 6 | PA6 | 0.4 | 24 | 0.4 | 8 |
| 7 | PA7 | 0.4 | 24 | 0.4 | 12 |



https://doi.org/10.1021/acsomega.4c01721
ACS Omega 2024, 9, 21401−21415

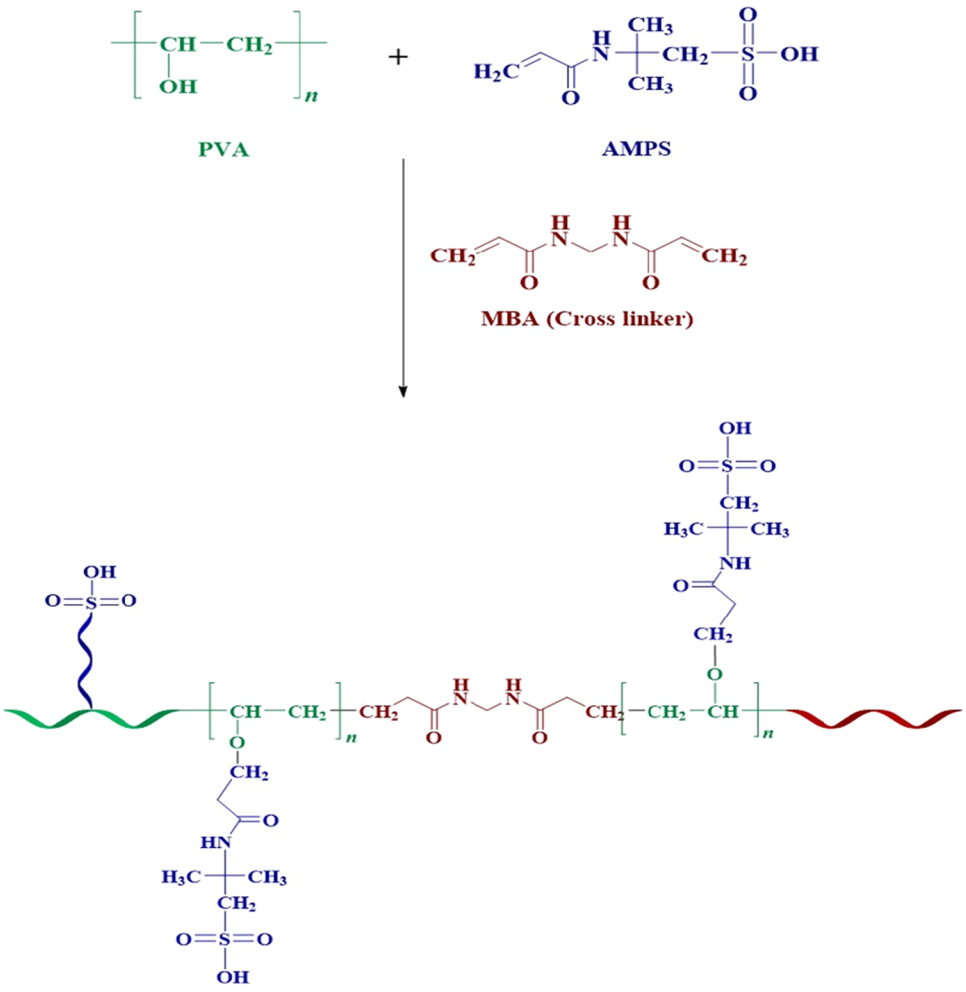


**Figure 1.** Possible structure of the crosslinked nanogels.

this, a solution of the drug (ticagrelor) was prepared in a methanol and water (1:1) mixture. An accurately weighed quantity of the nanogel was then added to the drug solution followed by sonication for 20 min. The sonicated drug−nanogel mixture was placed on a magnetic stirrer at 200 rpm for 24 h at 25 °C ± 1. After a specified time period, nanogels loaded with the drug were collected, dried at ambient temperature, and lyophilized. Then, the dried drug-loaded nanogels were investigated through physical and chemical characterizations.

**2.3. Characterization.** *2.3.1. Particle Size Analysis.* The particle size, $\zeta$-potential, and polydispersity index (PDI) were recorded for the optimum formulation of the synthesized PVA-*g*-poly (AMPS) nanogels by diluting (dispersing) a specific amount of the formulation in methanol and analyzed through a particle size analyzer (Malvern Zeta Sizer, U.K.).[4d]

*2.3.2. Fourier Transform Infrared Spectroscopy.* Fourier transform infrared (FTIR) spectroscopy was performed to confirm the synthesis of TGR-loaded nanogels, determine functional groups, and identify the interactions among various formulation excipients and the drug. For this purpose, spectra of the polymer (PVA), monomer (AMPS), pure drug (TGR), and unloaded and TGR-loaded nanogels were recorded at a resolution of 4 $cm^{-1}$ in the scanning range of 4000−500 $cm^{-1}$ by using an FTIR spectrometer (Nicolet Nexus) equipped with the attenuated total reflectance technique.[24]

*2.3.3. Thermal Analysis.* The thermal stability of the pure drug (TGR), polymer (PVA), monomer (AMPS), and unloaded and TGR-loaded nanogels was determined by thermogravimetric analysis (TGA) and differential scanning calorimetry (DSC) using a thermogravimetric analyzer (SDT 650 series). Accurately weighed samples (2−3 mg) were sealed in an aluminum pan, and analysis was performed in the temperature range of 0−500 °C with a heating rate of 10 °C $min^{-1}$ under a nitrogen atmosphere, maintaining a flow rate of 10 mL $min^{-1}$ to prevent thermo-oxidative degradation. Finally, the % loss of sample weight on increasing the temperature and exothermic and endothermic events were noted.[25]

*2.3.4. Powder X-ray Diffraction (PXRD) Analysis.* Powder X-ray diffraction (PXRD) was performed to determine the crystalline or amorphous nature of pure ingredients and blank and loaded nanogels at room temperature with an X-ray diffractometer (JDX3522, Japan). Specific amounts of samples were poured onto plastic sample holders, and the surface was leveled with a glass slide. XRD was carried out in the $2\theta$ (diffraction angle) range of 0−50° using 1.540 Å wavelength and Ni-filtered radiation from a Cu k$\alpha$ source.[26]

*2.3.5. Scanning Electron Microscopy.* The topography and morphology of the synthesized nanogels were observed with a scanning electron microscope (Hitachi S-2380-N, Tokyo, Japan). Completely dried nanogels were placed on a metal stub with double adhesive tape, sputter coated with a gold layer of 10 nm thickness, and examined under a high-resolution



https://doi.org/10.1021/acsomega.4c01721
ACS Omega 2024, 9, 21401−21415

electron microscope. Then, images were recorded at various magnifications.[27]

*2.3.6. In vitro Swelling Studies.* Swelling studies of the developed nanogels were carried out in distilled water and solutions of pH 1.2 (HCl buffer) and pH 6.8 (phosphate buffer). A literature-reported tea bag method was used.[42] To previously weighed empty tea bags, a known amount of dried nanogels was filled and submerged in beakers containing distilled water and solutions of pH 1.2 and 6.8 at 37 ± 1 °C. Tea bags were taken out from beakers after 2, 5, 10, 15, 20, 30, 45, 60, 90, and 120 min. The exterior of the bags was gently wiped with blotting paper and kept in the hanging position until no droplets were exuding from the bag. Using a weighing balance, the weight of the swollen particles was noted. Then, the bags were again soaked in the respective beakers. The same process of soaking and weighing was continued until a constant weight was achieved. Finally, the swelling index was calculated using eq 1

$$\text{swelling index} = \frac{W_2 - W_1}{W_1} \tag{1}$$

where $W_1$ and $W_2$ are the weights of nanogels at the initially dried and swollen states, respectively.

*2.3.7. Drug Entrapment Efficiency.* In order to quantify the drug entrapped in loaded nanogels, the extraction and absorption method was used.[28] A specified amount of the nanogel loaded with the drug (TGR) was accurately weighed and transferred to a mixture of methanol and distilled water (1:1). This mixture was placed on a magnetic stirrer adjusted at 200 rpm for 2 h at 25 °C ± 1. Then, the supernatant was removed and passed through a membrane filter having a pore size of 0.45 μm and examined spectrophotometrically at 255 nm ($\lambda_{max}$). From the calibration curve, the drug concentration was calculated. Finally, the % drug entrapment efficiency (% DEE) was calculated using eq 2

$$\%\text{DEE} = \frac{\text{actual amount of drug in nanogel}}{\text{theoretical amount of drug in nanogel}} \times 100 \tag{2}$$

*2.3.8. Solubility Studies.* Improving the solubility of hydrophobic drugs in the synthesized nanogels is a key parameter to be considered during characterization. For this purpose, solubility studies were executed in distilled water and solutions of pH 1.2 (HCl buffer) and pH 6.8 (phosphate buffer). The pure drug (TGR) and TGR-loaded nanogel formulations were added in small increments of 5 mL each to distilled water and solutions of pH 1.2 and pH 6.8 in Falcon tubes separately and vortexed for 5 min until the saturated solution was obtained. Then, all Falcon tubes were dipped in a mechanically shaking water bath adjusted at 37 °C for 72 h. After shaking, all mixtures were centrifuged at 6000 rpm for 30 min, and the supernatant was filtered through a membrane filter having 0.45 μm pore size. Suitable dilutions of filtrates were analyzed at 255 nm ($\lambda_{max}$) using a ultraviolet−visible (UV−vis) spectrophotometer. The drug concentration was determined from the calibration curve, and the solubility was calculated.[29]

*2.3.9. In Vitro Drug Release Studies.* The dissolution profile of TGR-loaded nanogel formulations was assessed in distilled water and solutions of pH 1.2 (HCl buffer) and pH 6.8 (phosphate buffer). Release studies were performed by using USP Dissolution Apparatus II maintained at 37 ± 0.5 °C °C and a stirring speed adjusted at 50 rpm. Precisely weighed amounts of drug-loaded nanogels were introduced into 500 mL each of distilled water and solutions of pH 1.2 and pH 6.8. After predefined time intervals, 5 mL of samples were withdrawn from each medium and replenished with an equivalent volume of fresh dissolution medium. Each withdrawn sample was passed through a cellulose membrane (0.45 μm pore diameter) followed by spectrophotometric analysis at 255 nm $\lambda_{max}$ to estimate drug release. To compare the drug release profile of the synthesized nanogel formulations, release studies were also performed with a commercially available TGR tablet (Virata).[30]

*2.3.10. Drug Release Kinetic Modeling.* The release kinetics of the drug from TGR-loaded nanogels was explored by applying mathematical models to the % drug release *vs* time data. The drug release data were computed using DD solver, an Excel add-in module.[31] The drug release behavior of the synthesized nanogels was analyzed by various kinetic models, *i.e.*, zero-order, first-order, Higuchi, and Korsmeyer−Peppas models, using eqs 3−6, respectively.

$$Q_t = K_0 t \tag{3}$$

where $Q_t$ is the amount of drug at time $t$ and $K_0$ is the zero-order rate constant.

$$\log Q_t = \log Q_0 K_1 t \tag{4}$$

where $Q_t$ is the amount of drug at time $t$, $Q_0$ is the amount of drug at time zero, and $K_1$ is the first-order rate constant.

$$Q_t = K_H t^{1/2} \tag{5}$$

where $Q_t$ is the amount of drug at time $t$ and $K_H$ is the Higuchi constant.

$$M_t/M_\infty = K_{kp} t^n \tag{6}$$

where $M_t$ and $M_\infty$ are the amounts of drug released at times $t$ and ∞, $K_{kp}$ is the Korsmeyer−Pappas constant, and $n$ is the release exponent.

*2.3.11. Cell Viability Assay.* To determine the cellular toxicity of the synthesized nanogels, a cell viability assay was carried out using a previously described thiazolyl blue tetrazolium bromide (MTT) test on a Caco-2 cell line.[32] Caco-2 is an immortalized human colorectal cell line, which is commonly used as an *in vitro* model for assessing drug toxicity. Caco-2 cells were seeded into 96-well plates at a density of 30,000 cells per well in Dulbecco's modified Eagle medium (DMEM) supplemented with 10% fetal bovine serum (FBS) and incubated to reach confluence. After seeding, cells were cultured in FBS-free DMEM media, treated with 0.5% dispersions of test samples, and incubated for periods of 6 and 24 h. After a specified duration, cells were carefully rinsed with phosphate buffer saline (PBS) once. After cleansing, cells were re-incubated for 1 h in FBS-free DMEM media supplemented with 500 μL of MTT solution. After 1 h, the supernatant was removed and fed with 500 μL of dimethyl sulfoxide (DMSO) to solubilize formazan (converted dye), and the absorbance was noted at 570 nm. Finally, the % viability of cells was determined using eq 7

$$\text{cell viability (\%)} = \frac{A_s}{A_d} \times 100 \tag{7}$$



https://doi.org/10.1021/acsomega.4c01721
ACS Omega 2024, 9, 21401−21415

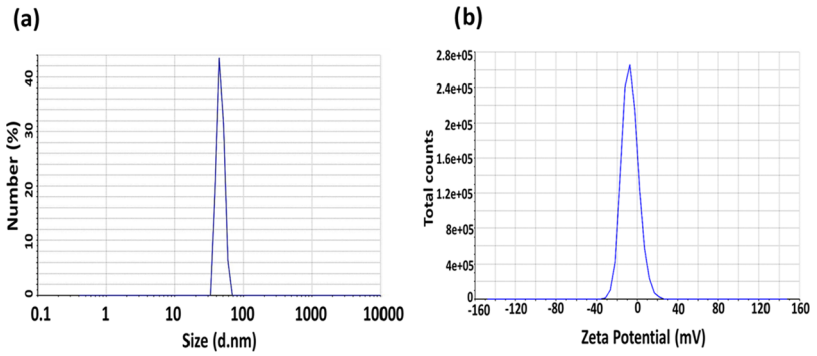


**Figure 2.** Particle size of PVA-*g*-poly (AMPS) nanogels (a) and ζ-potential measurement of PVA-*g*-poly (AMPS) nanogels (b).

where $A_s$ and $A_d$ are the absorbance values of cell cultures treated with test samples and untreated cell cultures (control), respectively.

*2.3.12. Oral Toxicity Studies.* The biocompatibility of the synthesized nanogels was ascertained by acute oral toxicity studies. To conduct the toxicity studies, guidelines of the Economic Co-operation and Development (OECD) were followed, and the Ethics Review Committee of Government College University Faisalabad, Pakistan (GCUF/ERC/354), thoroughly reviewed and approved the experimental protocol. Nine healthy albino rats weighing in the range of 200−250 g were procured from the Animal House Facility of Government College University Faisalabad, Pakistan. Rats were accommodated in neat, clean, and well-ventilated wooden cages with free approach to water and meal. The appropriate temperature (25 ± 2 °C) and relative humidity (65 ± 5%) were maintained in the quarantine area. Before commencing the study, rats were acclimatized for a duration of 1 week. The rats were distributed into 3 groups at random, *i.e.*, 3 in each group. Group 1 was designated as the control and was given normal saline intragastrically. Groups 2 and 3 were administered suspensions of unloaded nanogels and TGR-loaded nanogels, respectively, by the intragastric route. A total dose of 2000 mg/kg body weight was administered orally. All animals were fasted for 12 h before the dose was administered. The study was continued for 2 weeks. During the study period, all animals were closely monitored for mortality, morbidity, and general conditions including behavioral response, alertness, lacrimation, salivation, touch response, hair, feces, body weight, and any other significant clinical manifestations. On the 15th day, rats were exsanguinated for hematological analysis. The rats were then humanely euthanized, and vital internal organs were removed and submerged in 10% neutral buffered formalin (NBF) for preservation. The slides were made from thin tissue slices of organs and stained with hematoxylin and eosin dyes. The stained slides were microscopically observed for histopathological examination, and high-resolution images were obtained.

## 3. RESULTS AND DISCUSSION

**3.1. Particle Size Analysis.** Estimating the particle size of nanogels is of fundamental importance in terms of drug dissolution, solubility, and release. Particle size and solubility are inversely related to each other, as indicated by the Ostwald−Freundlich equation.[33] The results of the particle size distribution are depicted in Figure 2(a). The mean particle diameter was found to be 45.86 nm, with a PDI value of 0.41. A lower value of PDI is desirable as it indicates little propensity of particles to form clusters. A ζ-potential value between −30 and +30 mV is considered to be an acceptable criterion for indicating the physical stability of a nanofluid.[34] A ζ-potential value of −7.04 mV was recorded for the optimum nanogel formulation, as shown in Figure 2(b), which confirmed the colloidal stability of the PVA-*g*-poly (AMPS) nanogels synthesized by us.

**3.2. Fourier Transform Infrared (FTIR) Spectroscopy.** The FTIR spectra of PVA, AMPS, unloaded nanogels (PA5), ticagrelor (TGR), and TGR-loaded nanogels (PA5) were recorded to indicate crosslinking between the monomer (AMPS) and polymer (PVA) and also to investigate any interaction among drugs and excipients (Figure 3). The FTIR

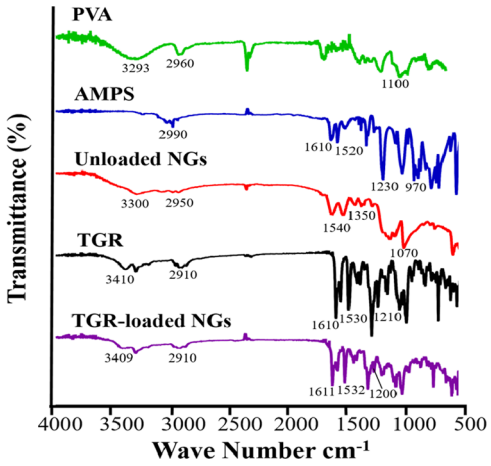


**Figure 3.** FTIR spectra of PVA, AMPS, unloaded nanogels, pure drug (TGR), and TGR-loaded nanogels.

spectrum of PVA exhibited absorption peaks at 3293.51, 2960.78, 1100.40, and 1030.18 $cm^{-1}$. The pinnacles at 3293.51 and 2960.78 $cm^{-1}$ specified the presence of −OH stretching and −CH extending vibrations, while the peak at 1100.40 $cm^{-1}$ pointed toward extended −C−O vibrations. The characteristic band at 1030.18 $cm^{-1}$ reflected the −C−OH stretching.[22c35] The IR spectrum of AMPS showed that the principle absorption peaks at 2990.70 and 1610.58 $cm^{-1}$ indicated −CH stretching of $-CH_2$ and carbonyl (-C═O) extending vibrations, respectively. The band at 1520.89 $cm^{-1}$ corresponded to −N−H bending vibrations. The presence of a sulfoxide (S═O) group is reflected by peaks at 1230.60 $cm^{-1}$ (symmetric stretching) and 1370.44 $cm^{-1}$ (asymmetric stretching). The characteristic pinnacles ranging between 1090 and 970 $cm^{-1}$ indicated the −S−O−C− group.[21,23] Figure 3 demonstrates that evident bands of AMPS and PVA


https://doi.org/10.1021/acsomega.4c01721
ACS Omega 2024, 9, 21401−21415

were slightly displaced in the spectrum of unloaded nanogels because of electrostatic interactions among different functional groups present in AMPS and PVA, resulting in the formation of a crosslinked structure. The peaks of AMPS at 2990.70 $cm^{-1}$ (−CH stretch) and PVA at 2960.78 $cm^{-1}$ (−CH stretch) overlapped at 2950.17 $cm^{-1}$. The bands of PVA at 3293.51 $cm^{-1}$ (−OH stretch), 1100.40 $cm^{-1}$ (extending −C−O vibration), and 1030.18 $cm^{-1}$ (-C−OH stretch) were slightly shifted to 3300.26, 1095.58, and 1015.53 $cm^{-1}$, respectively. The bands observed at 1650.13, 1540.18, 1350.19, and 1070.51 $cm^{-1}$ in the IR spectrum of unloaded nanogels were due to a minor shifting of the 1610.58, 1520.89, 1370.44, and 1090 $cm^{-1}$ peaks of AMPS, respectively. The FTIR spectrum of the pure drug (TGR) displayed distinctive pinnacles at 3410.20 and 3290.61 $cm^{-1}$ specific to −NH and −OH stretching vibrations, respectively. The peaks at 2910.63 $cm^{-1}$ reflected the presence of an alkyl stretch (−CH). The bands at 1610.58 and 1530.54 $cm^{-1}$ indicated −N−H stretch, while the peak at 1440.85 $cm^{-1}$ showed a methyl bend, and the one at 1210.35 $cm^{-1}$ represented −C−OH stretching. The peculiar peaks at 1105.23 and 1055.08 $cm^{-1}$ suggested −C−O stretching vibrations.[22c36] The presence of nearly unchanged peaks of TGR at 3409.25, 3289.70, 2910.63, 1611.55, 1532.47, 1441.81, 1200.70, and 1050.25 $cm^{-1}$ in the drug-loaded nanogels confirm that there was no chemical interaction among drugs and excipients, and the drug was efficiently loaded in the synthesized nanogels. Our findings showed consensus with results previously described by Maria et al., who designed a copolymeric hydrogel by using gelatin, PVA, and AMPS for prolonged sitagliptin and metformin release.[20a]

**3.3. Thermal Analysis.** The thermal stability of PVA, AMPS, ticagrelor (TGR), unloaded nanogels (PA5), and TGR-loaded nanogels (PA5) was evaluated over a temperature range of 0−500 °C by performing thermogravimetric analysis (TGA) and differential scanning calorimetry (DSC), as shown in Figure 4. The TGA scan of PVA (Figure 4a) showed 6%

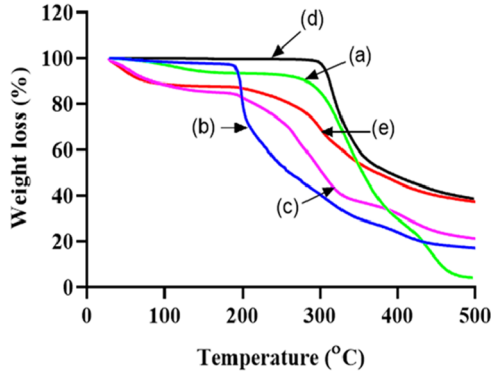


**Figure 4.** TGA thermograms of PVA (a), AMPS (b), unloaded nanogels (c), pure TGR (d), and TGR-loaded nanogels (e).

weight loss at temperatures up to 130 °C, which is attributed to water evaporation. Degradation started at 130 °C and lasted up to 295 °C, resulting in a 10% weight reduction. The major degradation phase extending from 295 to 500 °C contributed 75% reduction in weight. The degradation of PVA is linked with dehydration, leading to the formation of macromolecules with a polyene structure, which is further broken down at elevated temperatures to carbon and hydrocarbons.[37] The thermogram of AMPS (Figure 4b) exhibited three distinct degradation phases. The first phase between 0 and 195 °C resulted in a 5% reduction in weight due to the loss of moisture. The degradation during the second phase ensued between 195 and 210 °C and contributed 20% weight reduction due to the decomposition of the sulfonic acid group. The third degradation phase appeared at 210 °C and lasted until 500 °C, with 50% weight loss attributed to decomposition above its melting point.[20a21] TGA of pure TGR (Figure 4d) showed 3% weight loss at 301 °C due to the loss of residual moisture. Degradation at temperatures ranging from 301 to 340 °C and from 340 to 500 °C resulted in 42 and 17% weight loss, respectively. The TGA profile of unloaded nanogels (Figure 4c) demonstrated 15% weight loss at 190 °C. The next degradation stage observed at 260 °C resulted in a 17% weight reduction. Further degradation observed at 330−500 °C contributed to 46% weight loss. The TGA of unloaded nanogels exhibited that degradation of unloaded nanogels started slightly earlier but the decomposition was slower and lesser than those of PVA and AMPS. This indicated greater stability of the synthesized crosslinked nanogels than individual formulation components over the increased temperature range. In TGA of TGR-loaded nanogels (Figure 4e), weight loss was observed in three phases, *i.e.*, 12% up to 190 °C, 13% at temperatures ranging from 190 to 282 °C, and further 35% starting at 282 °C up to 500 °C. The percentage decomposition of TGR-loaded nanogels is comparable to the TGA of ticagrelor, but less than that of unloaded nanogels.

Figure 5 depicts the DSC curves of PVA, AMPS, TGR, and unloaded and TGR-loaded nanogels. In Figure 5a, PVA

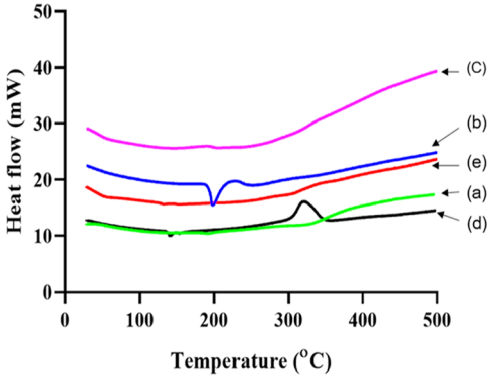


**Figure 5.** DSC thermograms of PVA (a), AMPS (b), unloaded nanogels (c), pure TGR (d), and TGR-loaded nanogels (e).

exhibited small endothermic dips at 85, 197, and 330 °C corresponding to the glass transition temperature, melting point, and thermal decomposition, respectively.[38] The DSC thermogram of AMPS (Figure 5b) exhibited an endothermic peak at 198 °C corresponding to its melting point. Another endothermic peak at 225 °C indicated thermal degradation.[28] In the DSC curve of unloaded nanogels (Figure 5c), individual melting point endothermic peaks of AMPS and PVA at 198 and 197 °C, respectively, overlapped at 210 °C. The disappearance of decomposition endothermic peaks of AMPS (at 225 °C) and PVA (at 330 °C) confirmed the thermal stability and amorphous nature of unloaded nanogels. The DSC scan of pure TGR (Figure 5d) shows an endothermic peak at 140 °C corresponding to its melting point, and the exothermic peak at 332 °C reveals its crystalline nature. In the DSC thermogram of TGR-loaded nanogels (Figure 5e), the


https://doi.org/10.1021/acsomega.4c01721
ACS Omega 2024, 9, 21401−21415

unshifted melting point peak of TGR (at 140 °C) confirmed the absence of chemical interactions between the drug and the synthesized nanogels. Also, the absence of an exothermic peak of TGR (at 332 °C) in the TGR-loaded nanogels confirmed the amorphous nature of the drug and its successful loading. Previously, Kifayat et al. reported similar findings when they prepared poloxamer-407 and AMPS-based nanogels with the aim of enhancing the solubility of olanzapine.[9a]

**3.4. Powder X-ray Diffraction (PXRD) Analysis.** The crystalline or amorphous features of PVA, AMPS, unloaded nanogels (PA5), ticagrelor (TGR), and TGR-loaded nanogels (PA5) were assessed by powder XRD analysis, as shown in Figure 6. PVA exhibited peaks at 2$\theta$ of 15.5 and 28°.[20a35] The

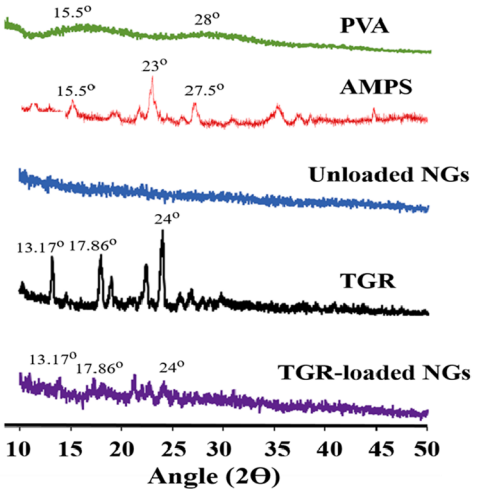


**Figure 6.** Powder X-ray diffraction patterns of PVA, AMPS, unloaded nanogels, pure drug (TGR), and TGR-loaded nanogels.

AMPS diffractogram displayed intense peaks at 2$\theta$ (diffraction angle) values of 11.5, 15.5, 19.5, 23, 26, and 27.5°, revealing its crystalline nature.[39] The diffractogram of pure TGR demonstrated intense peaks at 2$\theta$ of 13.17, 17.86, 18.98, 22.37, and 24°, confirming its crystalline nature.[22c40] The XRD spectrum of unloaded nanogels exhibited no characteristic sharp peak relevant to AMPS and PVA, which reflected its amorphous nature. Because of its amorphousness, the possibility of loading drugs in the synthesized nanogels was higher. The XRD spectrum of TGR-loaded nanogels presented all distinctive peaks of TGR with a remarkably diminished intensity, indicating the significantly reduced crystallinity and successful loading of the drug in nanogels. Consequently, it can be stated that the synthesized amorphous nanogel formulations masked the crystalline feature of the drug by means of a crosslinked network leading to efficient loading, enhanced solubility, and release of the drug. These outcomes conform to previously described observations by Minhas et al., who synthesized poly(vinylpyrrolidone) K-30-based nanogels in an attempt to improve the solubility of olanzapine.[12c]

**3.5. Scanning Electron Microscopy.** PVA-*g*-poly (AMPS) crosslinked nanogels were evaluated by scanning electron microscopy (SEM) analysis to interpret the surface morphology. Figure 7 shows the SEM images obtained at different magnification powers. Micrographs showed that the synthesized nanogels are irregular in shape and have a pitted, rough, and spongy appearance. The presence of several apertures on the entire surface is possibly ascribed to ionizable and hydrophilic groups of PVA and AMPS. The porous nature of the synthesized nanogels is favorable for water entrance, nanogel swelling, and subsequent drug loading and release. Shoukat et al. mentioned similar observations when they prepared hybrid nanogels from $\beta$-cyclodextrin, poly-(vinylpyrrolidone), and AMPS to counter the low solubility of rosuvastatin.

**3.6. *In Vitro* Swelling Studies.** Evaluating the swelling potential of nanogels is essential because it has a direct impact on the loading and release profile of the drug. The swelling index of the synthesized nanogels was investigated in distilled water and solutions of pH 1.2 (HCl buffer) and pH 6.8 (phosphate buffer). Prompt swelling was observed within the first 5 min due to hydrophilic monomers and polymers, nanodimensions, a large surface area, and spongy features of the particles, which facilitated rapid solution penetration. Figure 8a–c indicates that all nanogel formulations (PA1–PA7) exhibited substantial swelling in distilled water and both pH media, which is ascribed to the ionization of AMPS.[20a] Study outcomes revealed that the swelling was slightly more in pH 6.8 than in pH 1.2 and distilled water (Figure 8c). This is due to the sulfonate ions ($-SO_3^-$) present in AMPS, which were protonated to $-SO_3H$. Sulfonate groups robustly interacted with each other because of hydrogen bonding, which additionally crosslinked the nanogel network, resulting in hampered swelling in an acidic medium. In a basic medium, some sulfonate groups are ionized to sulfonate ions ($-SO_3^-$), leading to electrostatic repulsion between the anions, which resulted in the distancing of polymer chains, leading to increased swelling.[41] Further, the swelling index of nanogels as a function of ingredient concentration was also evaluated. With an increase in the polymer (PVA) concentration, the swelling decreased (Figure 8d) due to the formation of a tight network structure due to the crowding of polymer chains in the

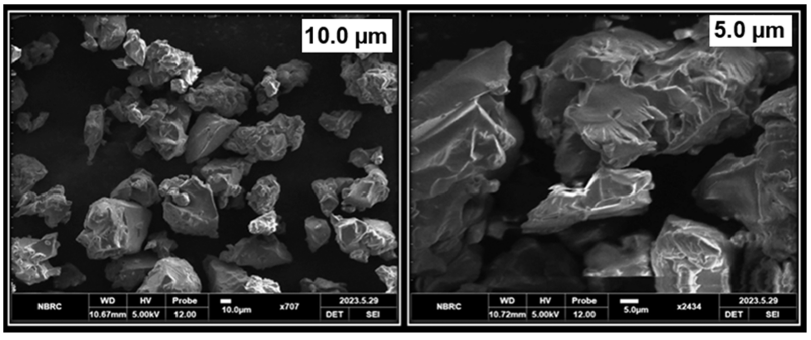


**Figure 7.** SEM micrographs of PVA-*g*-poly (AMPS) nanogels.



https://doi.org/10.1021/acsomega.4c01721
*ACS Omega* 2024, 9, 21401−21415

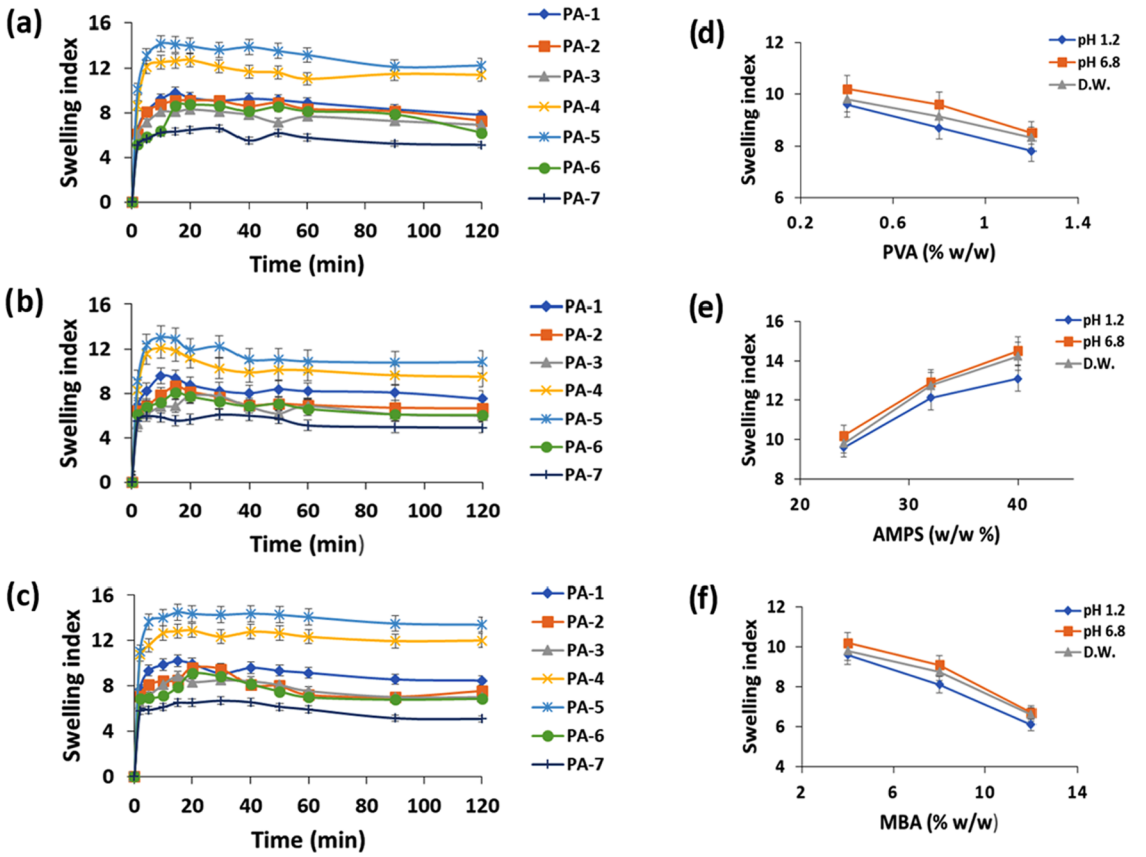


**Figure 8.** Swelling indices of PVA-*g*-poly (AMPS) nanogels in distilled water (a), at pH 1.2 (b), and at pH 6.8 (c); effect of the w/w % of PVA (d), AMPS (e), and MBA (f) on the swelling index of PVA-*g*-poly (AMPS) nanogels.

nanogel, which impeded the mobility and relaxation of the polymer chains, resulting in reduced water penetration.[42] An increase in swelling was observed by increasing the monomer (AMPS) concentration (Figure 8e). This is due to the hydrophilic nature and ionization of AMPS over a wide pH range, which further enhanced its hydrophilicity.[23,43] By increasing the feed composition of the crosslinker (MBA), the swelling was decreased (Figure 8f) due to excessive crosslinking, which resulted in intertwingled polymer chains, leading to a dense and firm network, which imparted some degree of hydrophobicity that protected the nanogel from immense water penetration.[40,44]

**3.7. Drug Entrapment Efficiency.** Drug-loaded nanogel formulations (PA1−PA7) with varying compositions were analyzed to estimate the drug entrapment efficiency. As illustrated in Figure 9, the drug entrapment efficiency (DEE) values ranged between 56.4 and 85.1%. Being hydrophilic in nature, the synthesized nanogels swell when they come in contact with aqueous media and entrap the drug. The entrapment efficiency decreased from 71.2 to 64.7% as the PVA concentration was gradually increased while keeping the AMPS and MBA concentrations constant, which is attributed to the formation of a dense structure due to the packing of the network by more polymer chains, which restrained chain relaxation and swelling.[42] When the concentration of AMPS was increased while keeping the PVA and MBA contents constant, the entrapment efficiency increased from 71.2 to 85.1%. This might be due to the presence of a large number of sulfonate ions ($-SO_3^-$) formed by the ionization of AMPS. The electrostatic repulsion between sulfonate ions causes the

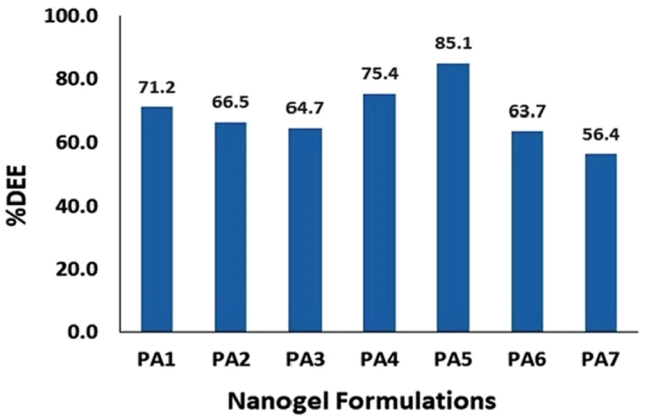


**Figure 9.** % Drug entrapment efficiency of different formulations (PA1−PA7).

widening of channels in the crosslinked network, resulting in greater porosity and swelling.[23] The %DEE was inversely related to the increasing MBA concentration in the formulation and decreased from 71.2 to 56.4% while maintaining fixed concentrations of PVA and AMPS, which is ascribed to the formation of a highly cross-connected and impervious network.[35] The maximum drug entrapment efficiency (85.1%) was observed in the formulation with the highest AMPS concentration (PA5). It is noteworthy that the results of entrapment efficiency are in line with swelling studies, as greater swelling leads to increased porosity and a higher drug entrapment capacity of the polymeric network.


https://doi.org/10.1021/acsomega.4c01721
ACS Omega 2024, 9, 21401−21415

Similar observations were reported by Sarfraz et al., who prepared a gastro-protective nanogel delivery system using carbopol and methacrylic acid for the successful delivery of ketoprofen.[45]

**3.8. Solubility Studies.** The solubility of the drug (TGR) in the pure form and from TGR-loaded nanogels (PA1−PA7) was evaluated in distilled water and solutions of pH 1.2 (HCl buffer) and pH 6.8 (phosphate buffer). As shown in Figure 10,

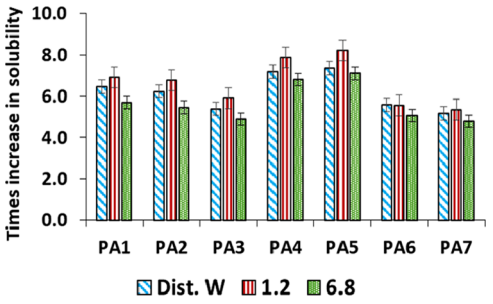


**Figure 10.** Solubility of drugs from nanogel formulations (PA1−PA7) in distilled water and buffer media of pH 1.2 and 6.8.

TGR-loaded nanogels substantially boosted the TGR solubility in comparison to that of the pure drug. The solubility of TGR in the synthesized nanogel formulations (PA1−PA7) increased 6.5, 6.2, 5.4, 7.2, 7.4, 5.6, and 5.2 times, respectively, in distilled water, while 5.7, 5.5, 5.3, 6.8, 7.1, 5.1, and 4.8 times, respectively, at pH 6.8. At pH 1.2, the TGR solubility of all formulations (PA1−PA7) increased by 6.9, 6.8, 5.9, 7.9, 8.2, 5.6, and 5.4-fold, respectively. The significantly improved solubility of TGR might be credited to the hydrophilicity, nanodimension, larger surface area, amorphous nature, porosity, efficient drug loading, and swellability of the synthesized nanogels and reduced crystallinity of TGR in nanogels, as also confirmed by XRD and DSC analyses. Our findings are in accordance with the outcomes of previous studies intended to improve the solubility of hydrophobic drugs by employing nanogels as drug delivery platforms.[4d9a12c23,46]

**3.9. *In Vitro* Drug Release Studies.** Dissolution studies were carried out in distilled water and solutions of pH 1.2 (HCl buffer) and pH 6.8 (phosphate buffer) to investigate drug release from nanogel formulations (PA1−PA7). To compare the drug release from the synthesized formulations with the reference product, dissolution studies were also conducted for the marketed brand of TGR (Virata). All synthesized formulations demonstrated a higher drug release, as shown in Figure 11. This is attributed to the reduced crystallinity of TGR in nanogels and nanosizing, hydrophilicity, and amorphousness of the synthesized formulations, which facilitated the prompt swelling of the crosslinked network and drug release. After the first 5 min, drug releases of 20.4−30.2, 17.2−35.3, and 14.5−30.9% were observed in distilled water, pH 1.2, and pH 6.8, respectively. This rapid release was due to the dissolution of loosely bound drugs on the outer surface of nanogels and also the rapid swelling of the polymeric network.

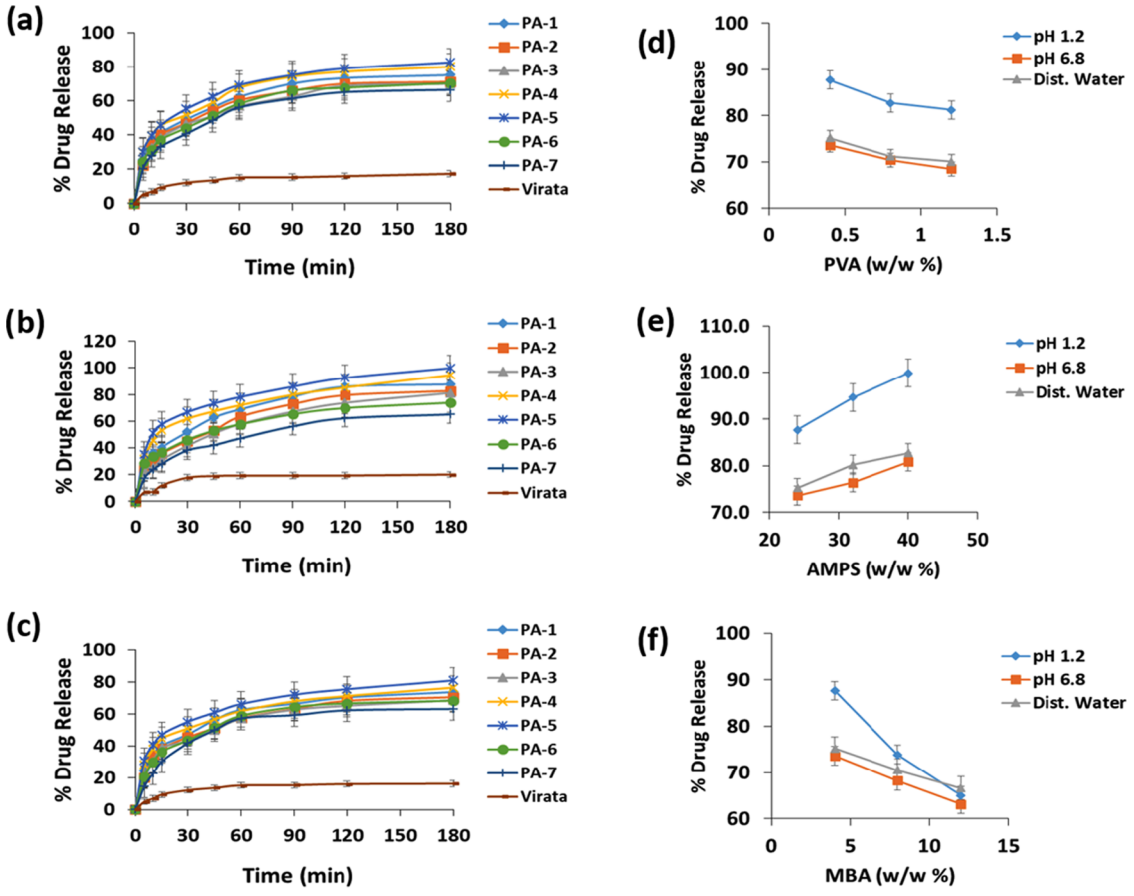


**Figure 11.** Percent drug release of nanogel formulations (PA1−PA7) and the marketed product (Virata) in distilled water (a), pH 1.2 (b), and pH 6.8 (c); effect of the % w/w of PVA (d), AMPS (e), and MBA (f) on drug release.



https://doi.org/10.1021/acsomega.4c01721
ACS Omega 2024, 9, 21401−21415

Table 2. Drug Release Kinetics Modeling of TGR-Loaded Nanogel Formulations (PA1−PA7)

| | | zero-order | first-order | Higuchi Model | Korsmeyer−Peppas model | |
|---|---|---|---|---|---|---|
| formulation code | pH | $R^2$ | $R^2$ | $R^2$ | $R^2$ | $n$ |
| PA1 | D.W. | 0.9091 | 0.9830 | 0.9732 | 0.9901 | 0.2466 |
| | 1.2 | 0.9136 | 0.9969 | 0.9771 | 0.9893 | 0.3181 |
| | 6.8 | 0.9052 | 0.9778 | 0.9725 | 0.9919 | 0.2497 |
| PA2 | D.W. | 0.8919 | 0.9679 | 0.9637 | 0.9862 | 0.2488 |
| | 1.2 | 0.9277 | 0.9981 | 0.9828 | 0.9902 | 0.3538 |
| | 6.8 | 0.9075 | 0.9674 | 0.9696 | 0.9869 | 0.2618 |
| PA3 | D.W. | 0.9259 | 0.9823 | 0.9818 | 0.9942 | 0.2492 |
| | 1.2 | 0.9466 | 0.9996 | 0.9912 | 0.9950 | 0.3792 |
| | 6.8 | 0.9060 | 0.9670 | 0.9705 | 0.9883 | 0.2617 |
| PA4 | D.W. | 0.9183 | 0.9918 | 0.9778 | 0.9917 | 0.2349 |
| | 1.2 | 0.9168 | 0.9716 | 0.9757 | 0.9921 | 0.2622 |
| | 6.8 | 0.9297 | 0.9840 | 0.9828 | 0.9960 | 0.2213 |
| PA5 | D.W. | 0.9129 | 0.9945 | 0.9778 | 0.9958 | 0.2386 |
| | 1.2 | 0.9097 | 0.9583 | 0.9725 | 0.9914 | 0.2497 |
| | 6.8 | 0.9108 | 0.9868 | 0.9754 | 0.9957 | 0.2106 |
| PA6 | D.W. | 0.9198 | 0.9837 | 0.9791 | 0.9916 | 0.2614 |
| | 1.2 | 0.9274 | 0.9986 | 0.9845 | 0.9954 | 0.2800 |
| | 6.8 | 0.8893 | 0.9653 | 0.9642 | 0.9855 | 0.2722 |
| PA7 | D.W. | 0.9115 | 0.9748 | 0.9757 | 0.9900 | 0.2852 |
| | 1.2 | 0.9275 | 0.9866 | 0.9839 | 0.9926 | 0.3538 |
| | 6.8 | 0.8460 | 0.9272 | 0.9384 | 0.9650 | 0.3113 |

After 180 min, the % drug release ranged from 66.6 to 82.7% in distilled water, from 65.03 to 99.9% at pH 1.2, and from 63.1 to 80.8% at pH 6.8. The higher release of TGR at pH 1.2 might be due to the basic character of the drug, which dissolved well in acidic pH.[22d]

The effect of increasing the concentration of excipients on drug release was also evaluated. On increasing the PVA concentration from 0.4 to 1.2%, the drug release decreased from 75.2 to 70.1% in distilled water, from 87.7 to 81.2% at pH 1.2, and from 73.6 to 68.5% at pH 6.8, as shown in Figure 11(d). This is attributed to the formation of a more dense structure by increasing the concentration, which inhibits polymer chain relaxation for water absorption, resulting in reduced swelling and consequently leading to less drug release.[42] The drug release was increased from 75.2 to 82.7% in distilled water, from 87.7 to 99.9% at pH 1.2, and from 73.6 to 80.8% at pH 6.8 when the AMPS concentration was increased from 24 to 40%, as shown in Figure 11(e). This is due to the fact that AMPS is ionizable at both pH values, and the production of a large number of sulfonate ions resulted in greater repulsion among polymeric chains, causing a widening of pores in the crosslinked network and facilitating water penetration and drug release.[20a] On increasing the crosslinker (MBA) concentration from 4 to 12%, a trend of decreasing drug release was noted from 75.2 to 66.6% in distilled water, from 87.7 to 65.03% at pH 1.2, and from 73.6 to 63.1% at pH 6.8, as shown in Figure 11(f). This is ascribed to the increased crosslinking density of the polymeric network resulting in reduced elasticity and porosity, leading to diminished swelling and drug release.[40]

The commercially available tablet (Virata) of TGR was also subjected to release studies. The results of studies show that the synthesized nanogels presented much higher drug release as compared to the TGR tablet (Virata). In distilled water, TGR-loaded nanogels released 82.7% drug in 180 min, whereas the ticagrelor tablet reached 17.3%, as illustrated in Figure 11(a). At pH 1.2, TGR-loaded nanogels reached 99.9% drug release in 180 min, whereas the ticagrelor tablet reached 20.1%, as depicted in Figure 11(b). At pH 6.8, TGR-loaded nanogels released 80.8% drug in 180 min, whereas the ticagrelor tablet released only 16.3% within the same duration, as shown in Figure 11(c). Similar inferences were made by Young et al., who synthesized a TPGS/PVA-based nanosuspension for enhancing the dissolution of ticagrelor.[22c] This remarkable difference in dissolution between the synthesized formulations and the reference product confirmed that our nanogels are promising delivery systems with respect to the enhancement of drug dissolution and release.

**3.10. Drug Release Kinetics Modeling.** The drug release kinetics were determined by applying the dissolution data to mathematical models (*i.e.*, zero-order, first-order, Higuchi, and Korsmeyer−Peppas). The zero-order kinetics explain the constant fraction of drug release per specific time period regardless of the initial or remaining concentration in the delivery vehicle, and when the release of a drug depends on the concentration present in the delivery system, it corresponds to first-order release. The results of kinetic models (Table 2) indicated that all formulations obeyed first-order kinetics of release. Moreover, dissolution data were obtained through the Higuchi and Korsmeyer−Peppas models to determine the mechanism of drug release. The Higuchi model assumes that the Fickian diffusion is the principle release mechanism, and the drug release process is dependent on the square root of time. The drug release from polymeric matrices such as nanogels is better explained by the Korsmeyer−Peppas model and is more applicable when the release follows a hybrid mechanism. The release exponent "$n$" is of utmost importance, as its value indicates the release mechanism. A value of $n \leq 0.43$ indicates that the Fickian diffusion is responsible for drug release, whereas a value of $0.43 < n < 0.85$ points toward anomalous drug release (non-Fickian) diffusion. Super case-II transport is the principle release mechanism for a value of $n > 0.85$. The results (Table 2) disclosed that the Korsmeyer−Peppas model is better fitted due to the higher coefficient of



https://doi.org/10.1021/acsomega.4c01721
ACS Omega 2024, 9, 21401−21415

correlation ($R^2$) value. All synthesized formulations (PA1−PA7) followed the Korsmeyer−Peppas model, with 'n' values less than 0.43, which revealed that the release mechanism was predominantly based on the Fickian diffusion.[47]

**3.11. Cell Viability Assay.** The cell viability assay is an essential technique used in the preclinical phases of the drug development process to examine the general health and phenotypic characteristics of cells when tested against pharmaceutical formulations. In the current work, the cell viability was assessed by an MTT assay, where Caco-2 cell cultures were treated with both unloaded and TGR-loaded nanogels. The cells of the control group were cultured using DMEM alone. The outcomes of the assay confirmed the noncytotoxic nature of the synthesized nanogels, as 83% of the cells remained alive when treated with both unloaded and drug-loaded nanogels for a duration of 24 h (Figure 12).

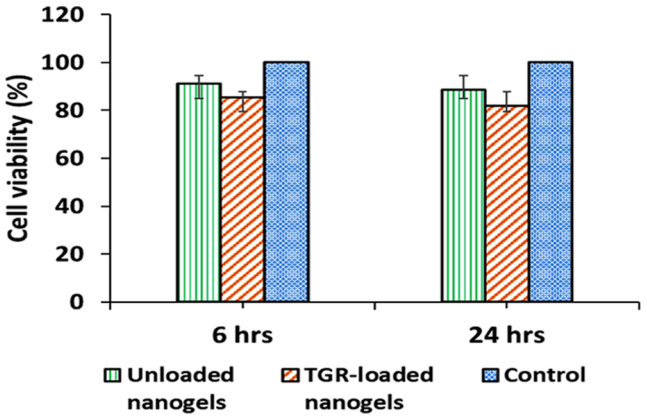


**Figure 12.** Cell viability study of unloaded and TGR-loaded nanogels.

Furthermore, the microscopic examination of cell lines showed no apparent change in the cellular morphology. Our observations were in good agreement with results reported by Iqbal et al., who developed nanoparticles using thiolated chitosan and Eudragit RS100 for the delivery of moxifloxacin in a controlled manner.[48]

**3.12. Oral Toxicity Studies.** The compatibility of the synthesized nanogel formulations with the biological environment was assessed by conducting acute oral toxicity studies in albino rats. The studies were evaluated by clinical, hematological, biochemical, and histopathological assessments. According to clinical manifestations, no mortality was observed in either the control (group 1) or treatment groups (groups 2 and 3). All animals of the control and treatment groups exhibited similar behavioral patterns and activities. There were no noticeable differences in the food and water intake, urination, touch and pain responses, and corneal and righting reflexes. Common ailments, such as eye lacrimation, inflammation, vomiting, diarrhea, and edema, were absent. These findings show that the synthesized formulations are clinically safe.

After 14 days, all animals were exsanguinated and later humanely euthanized for biochemical and histopathological examination. The physiological and pathological states are reflected by values of hematological markers. Various hematological parameters such as hemoglobin, erythrocyte (RBC) count with the mean corpuscular volume (MCV) and hematocrit (HCT) values, mean cell hemoglobin (MCH), total leukocyte count (TLC), and platelet count were determined, as shown in Table 3. The results of other hematological tests such as serum urea and creatinine,

**Table 3. Values of Hematological Parameters of the Control and Treatment Groups**

| sr., no. | parameter | group 1 (control) | group 2 (treated with unloaded nanogels) | group 3 (treated with TGR-loaded nanogels) |
|---|---|---|---|---|
| 1 | hemoglobin (g/dl) | 13.7 | 14.5 | 13.8 |
| 2 | total RBCs ($\times 10^6/\mu L$) | 6.73 | 7.57 | 6.87 |
| 3 | HCT (%) | 44.9 | 42.9 | 45.8 |
| 4 | MCV (fl) | 66.7 | 67.2 | 66.1 |
| 5 | MCH (Pg) | 17.4 | 19.1 | 18.5 |
| 6 | MCHC (%) | 26.1 | 26.8 | 25.2 |
| 7 | TLC ($\times 10^3/\mu L$) | 8.2 | 9.8 | 8.5 |
| 8 | neutrophils (%) | 21.3 | 20.5 | 18 |
| 9 | lymphocytes (%) | 65.7 | 60.4 | 68.2 |
| 10 | monocytes (%) | 4 | 6 | 5 |
| 11 | eosinophils (%) | 2 | 3 | 2 |
| 12 | platelet count ($\times 10^3/\mu L$) | 1110 | 1009 | 1090 |

aspartate transferase (AST), alanine aminotransferase (ALT), bilirubin, cholesterol, and triglycerides (TG) are also reported in Table 4. All hematological parameters were in the normal

**Table 4. Results of RFTs, LFTs, and Lipid Profiles of the Control and Treatment Groups**

| sr., no. | biochemical analysis | group 1 (control) | group 2 (treated with unloaded nanogels) | group 3 (treated with TGR-loaded nanogels) |
|---|---|---|---|---|
| 1 | serum urea (mg/dl) | 18.1 | 19.2 | 18.7 |
| 2 | serum creatinine (mg/dl) | 0.6 | 0.51 | 0.57 |
| 3 | AST (IU/L) | 92 | 87 | 94 |
| 4 | ALT (IU/L) | 35 | 39 | 37 |
| 5 | bilirubin (mg/dl) | 0.6 | 0.7 | 0.6 |
| 6 | cholesterol (mg/dl) | 62.3 | 65.1 | 64.5 |
| 7 | triglycerides (mg/dl) | 95.6 | 94.8 | 99.1 |
| 8 | HDL (mg/dl) | 26.7 | 25.4 | 29.7 |
| 9 | LDL (mg/dl) | 58.3 | 60.7 | 58.8 |

range in the treatment (groups 2 and 3) and control (group 1) groups. The results of the hematological analysis confirm the safety of the synthesized nanogel formulations with no evidence of nephrotoxicity and hepatotoxicity.

The effect of the synthesized formulations on the weights of vital internal organs was also evaluated. The organ weights of animals in the control and treatment groups did not differ noticeably (Table 5). Microscopic examination of the tissue sections of vital organs was also carried out. No signs of lesions, inflammation, or abnormality were detected in animals of either the control or treatment groups, as shown in Figure 13. No sign of pathological change was observed within


https://doi.org/10.1021/acsomega.4c01721
ACS Omega 2024, 9, 21401−21415

**Table 5. Weights of Vital Internal Organs of Rats from the Control and Treatment Groups**

| sr., no. | body organs (gm) | group 1 (control) | group 2 (treated with unloaded nanogels) | group 3 (treated with TGR-loaded nanogels) |
|---|---|---|---|---|
| 1 | heart | 0.87 ± 0.2 | 0.89 ± 0.1 | 0.88 ± 0.2 |
| 2 | lungs | 1.93 ± 0.1 | 1.93 ± 0.2 | 1.91 ± 0.2 |
| 3 | liver | 7.72 ± 0.3 | 7.81 ± 0.1 | 7.82 ± 0.0 |
| 4 | kidneys | 1.88 ± 0.0 | 1.91 ± 0.1 | 1.86 ± 0.3 |
| 5 | stomach | 1.97 ± 0.1 | 2.01 ± 0.2 | 1.95 ± 0.2 |
| 6 | small intestine | 0.61 ± 0.1 | 0.62 ± 0.3 | 0.64 ± 0.1 |
| 7 | brain | 2.201 ± 0.2 | 2.18 ± 0.3 | 2.21 ± 0.4 |
| 8 | spleen | 0.57 ± 0.1 | 0.59 ± 0.2 | 0.56 ± 0.3 |

cardiomyocytes. The lungs did not show any alveolar damage, and hepatic parenchyma was normal, with no damage to hepatocytes. Microscopic examination of the kidney revealed a normal glomerulus connected to the Bowman's capsule. The gastric mucosa was free of any sign of ulceration. The intestinal brush border layer was intact, with clearly visible microvilli. On histological examination of the brain, neurons appeared normal without any damage to axons, and the spleen showed normal features with unchanged white and red pulps. On compiling the results obtained from toxicity studies, it can be concluded that the synthesized nanogel formulations are well-tolerated, nontoxic, and biocompatible when administered orally. Similar toxicity study findings were reported by Qandeel et al, who synthesized $\beta$-cyclodextrin-based nanosponges for the solubility enhancement of dexibuprofen.[49]

## 4. CONCLUSIONS

Poor solubility is a serious setback to adequate oral bioavailability and therapeutic outcomes of the majority of the marketed drugs and drugs under developmental stages. In the current work, this issue was addressed by developing PVA-*g*-poly(AMPS) nanogels using a free radical polymerization technique for enhancing the solubility of the poorly soluble drug ticagrelor (TGR). The synthesized nanogels exhibited particle sizes in the desired range with a high swelling index and drug entrapment efficiency. XRD analysis indicated the highly amorphous nature of the synthesized nanogels and markedly declined crystallinity of TGR, which are of prime importance in the case of solubility enhancement. FTIR and thermal analyses confirmed the formation of a stable formulation without any interaction among drugs and excipients. The solubility of TGR in nanogels was enhanced up to 8.2-fold, and the *in vitro* dissolution was significantly

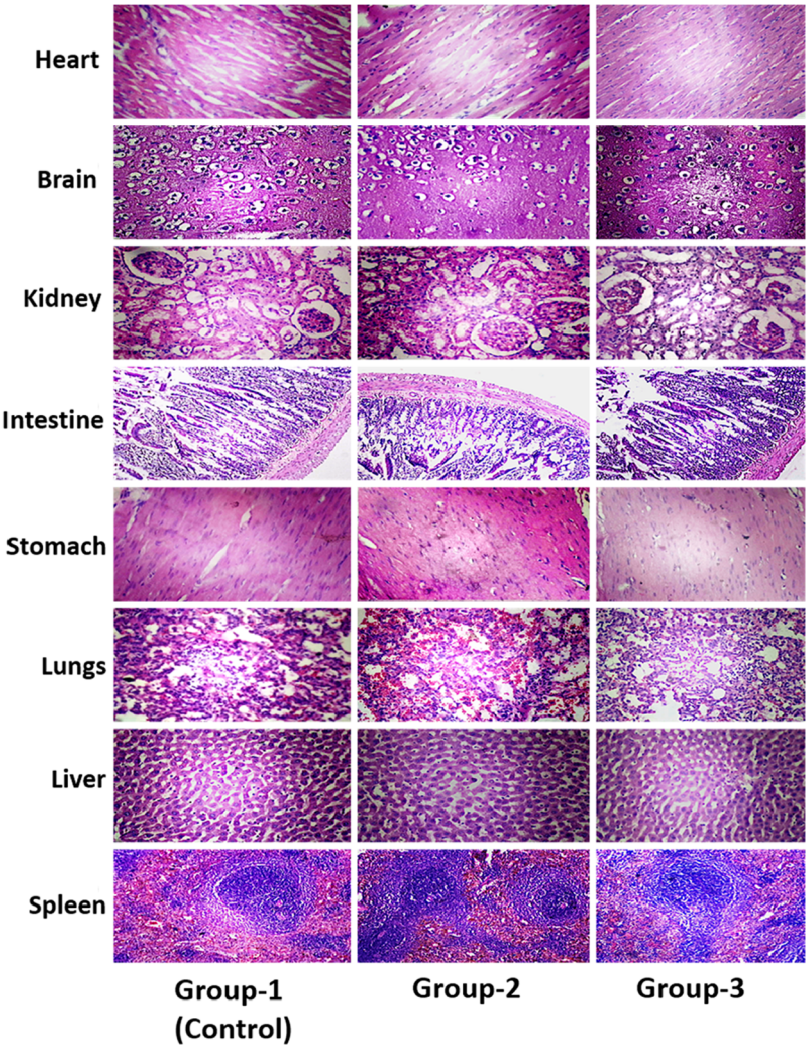


**Figure 13.** Histological examination of vital organs of rats in the control and treatment groups.



https://doi.org/10.1021/acsomega.4c01721
*ACS Omega* 2024, 9, 21401−21415

higher and expeditious compared to that of the marketed product (Virata). Oral toxicity studies in rats and the MTT assay confirmed the safety and biocompatibility of the synthesized nanogels. Hence, the synthesized PVA-*g*-poly-(AMPS) nanogels offer prospective pharmaceutical delivery systems for improving the solubility and dissolution of TGR and other poorly soluble drugs.

## AUTHOR INFORMATION


### Corresponding Author

**Ikrima Khalid** − *Department of Pharmaceutics, Faculty of Pharmaceutical Sciences, Government College University, Faisalabad 38000, Pakistan*; Phone: 0092-345-8730002; Email: ikrima_khalid@yahoo.com

### Authors

**Usman Saleem** − *Department of Pharmaceutics, Faculty of Pharmaceutical Sciences, Government College University, Faisalabad 38000, Pakistan*; orcid.org/0009-0002-8867-9363

**Liaqat Hussain** − *Department of Pharmacology, School of Medicine and Public Health, Zhejiang University, Hanzghou 310027, China; Department of Pharmacology, Faculty of Pharmaceutical Sciences, Government College University, Faisalabad 38000, Pakistan*

**Abdulrahman Alshammari** − *Department of Pharmacology and Toxicology, College of Pharmacy, King Saud University, Riyadh 11451, Saudi Arabia*

**Norah A. Albekairi** − *Department of Pharmacology and Toxicology, College of Pharmacy, King Saud University, Riyadh 11451, Saudi Arabia*

Complete contact information is available at: https://pubs.acs.org/10.1021/acsomega.4c01721


### Notes

The authors declare no competing financial interest.

## ACKNOWLEDGMENTS

The authors are thankful to the researchers supporting project number (RSP2024R491), King Saud University, Riyadh, Saudi Arabia.

## REFERENCES


(1) Jermain, S. V.; Brough, C.; Williams, R. O., III Amorphous solid dispersions and nanocrystal technologies for poorly water-soluble drug delivery−an update. *Int. J. Pharm.* **2018**, *535* (1−2), 379−392.

(2) Ambrus, R.; Szabó-Révész, P.; Kiss, T.; Nagy, E.; Szűcs, T.; Smausz, T.; Hopp, B. Application of a suitable particle engineering technique by pulsed laser ablation in liquid (PLAL) to modify the physicochemical properties of poorly soluble drugs. *J. Drug Delivery Sci. Technol.* **2020**, *57*, No. 101727.

(3) (a) Alshweiat, A.; Csóka, I.; Tömösi, F.; Janáky, T.; Kovács, A.; Gáspár, R.; Sztojkov-Ivanov, A.; Ducza, E.; Márki, Á.; Szabó-Révész, P.; Ambrus, R. Nasal delivery of nanosuspension-based mucoadhesive formulation with improved bioavailability of loratadine: preparation, characterization, and *in vivo* evaluation. *Int. J. Pharm.* **2020**, *579*, No. 119166. (b) Mao, J.; Wang, H.; Xie, Y.; Fu, Y.; Li, Y.; Liu, P.; Du, H.; Zhu, J.; Dong, L.; Hussain, M.; et al. Transdermal delivery of rapamycin with poor water-solubility by dissolving polymeric microneedles for anti-angiogenesis. *J. Mater. Chem. B* **2020**, *8* (5), 928−934. (c) Liu, T.; Yu, X.; Yin, H. Study of top-down and bottom-up approaches by using design of experiment (DoE) to produce meloxicam nanocrystal capsules. *Aaps PharmScitech* **2020**, *21*, No. 79. (d) Kara, D. D.; Rathnanand, M. Cocrystals and Drug−Drug Cocrystals of Anticancer Drugs: A Perception towards Screening Techniques, Preparation, and Enhancement of Drug Properties. *Crystals* **2022**, *12* (10), No. 1337. (e) Mohandoss, S.; Velu, K. S.; Stalin, T.; Ahmad, N.; Alomar, S. Y.; Lee, Y. R. Tenofovir antiviral drug solubility enhancement with *β*-cyclodextrin inclusion complex and in silico study of potential inhibitor against SARS-CoV-2 main protease (Mpro). *J. Mol. Liq.* **2023**, *377*, No. 121544.

(4) (a) Navarro, L.; Theune, L. E.; Calderon, M. Effect of crosslinking density on thermoresponsive nanogels: A study on the size control and the kinetics release of biomacromolecules. *Eur. Polym. J.* **2020**, *124*, No. 109478. (b) Mahmood, A.; Ijaz, H.; Sarfraz, R. M.; Zafar, N.; Zaman, M.; Azam, M. Polymeric Hydrogels and Nanogels: Classification, Development, and Pharmaceutical Applications. In *Hydrogels and Nanogels - Applications in Medicine*; IntechOpen, 2023. (c) Yadav, H.; Anwar, N.; Halabi, A.; Alsalloum, G. Nanogels as Novel Drug delivery Systems-a Review Properties of Nanogels Keywords: Introduction Advantages of Nanogels. *Insight Pharm. Res.* **2017**, *1* (5), 1−8. (d) Khan, K. U.; Minhas, M. U.; Sohail, M.; Badshah, S. F.; Abdullah, O.; Khan, S.; Munir, A.; Suhail, M. Synthesis of PEG-4000-co-poly (AMPS) nanogels by cross-linking polymerization as highly responsive networks for enhancement in meloxicam solubility. *Drug Dev. Ind. Pharm.* **2021**, *47* (3), 465−476.

(5) Suhail, M.; Rosenholm, J. M.; Minhas, M. U.; Badshah, S. F.; Naeem, A.; Khan, K. U.; Fahad, M. Nanogels as drug-delivery systems: A comprehensive overview. *Ther. Delivery* **2019**, *10* (11), 697−717.

(6) (a) Ali, A.; Khalid, I.; Minhas, M. U.; Barkat, K.; Khan, I. U.; Syed, H. K.; Umar, A. Preparation and *in vitro* evaluation of Chondroitin sulfate and Carbopol based mucoadhesive controlled release polymeric composites of Loxoprofen using factorial design. *Eur. Polym. J.* **2019**, *121*, No. 109312. (b) Ullah, K.; Sohail, M.; Buabeid, M. A.; Murtaza, G.; Ullah, A.; Rashid, H.; Khan, M. A.; Khan, S. A. Pectin-based (LA-co-MAA) semi-IPNS as a potential biomaterial for colonic delivery of oxaliplatin. *Int. J. Pharm.* **2019**, *569*, No. 118557. (c) Ajaz, N.; Khan, I. U.; Khalid, I.; Khan, R. U.; Khan, H. A.; Asghar, S.; Khalid, S. H.; Shahzad, Y.; Yousaf, A. M.; Hussain, T.; et al. *In vitro* and toxicological assessment of dexamethasone sodium phosphate loaded pH sensitive Pectin-g-poly (AA)/PVP semi interpenetrating network. *Mater. Today Commun.* **2020**, *25*, No. 101325. (d) Hua, B.; Wei, H.; Hu, C.; Zhang, Y.; Yang, S.; Wang, G.; Guo, T.; Li, J. Preparation of pH/temperature-responsive semi-IPN hydrogels based on sodium alginate and humic acid as slow-release and water-retention fertilizers. *Polym. Bull.* **2023**, *81*, 4175−4198. (e) Suhail, M.; Hsieh, Y.-H.; Shao, Y.-F.; Minhas, M. U.; Wu, P.-C. Formulation and in-vitro characterization of pH-responsive semi-interpenetrating polymer network hydrogels for controlled release of ketorolac tromethamine. *Gels* **2021**, *7* (4), No. 167.

(7) Kendre, P. N.; Satav, T. Current trends and concepts in the design and development of nanogel carrier systems. *Polym. Bull.* **2019**, *76*, 1595−1617.

(8) Lee, K. Z.; Jeon, J.; Jiang, B.; Subramani, S. V.; Li, J.; Zhang, F. Protein-Based Hydrogels and Their Biomedical Applications. *Molecules* **2023**, *28* (13), No. 4988.

(9) (a) Khan, K. U.; Akhtar, N.; Minhas, M. U. Poloxamer-407-co-poly (2-acrylamido-2-methylpropane sulfonic acid) cross-linked nanogels for solubility enhancement of olanzapine: synthesis, characterization, and toxicity evaluation. *AAPS PharmSciTech* **2020**, *21*, No. 141. (b) Stawicki, B.; Schacher, T.; Cho, H. Nanogels as a versatile drug delivery system for brain cancer. *Gels* **2021**, *7* (2), No. 63.

(10) Cho, H. Nanogels for Locoregional Drug Delivery. In *Functional Nanocomposite Hydrogels*; Elsevier, 2023; pp 479−516.

(11) (a) Trotta, F.; Mele, A. *Nanosponges: Synthesis and Applications*; John Wiley & Sons, 2019. (b) Sun, X.-F.; Zeng, Q.; Wang, H.; Hao, Y. Preparation and swelling behavior of pH/temperature responsive semi-IPN hydrogel based on carboxymethyl xylan and poly (N-isopropyl acrylamide). *Cellulose* **2019**, *26*, 1909−1922. (c) Yiamsawas, D.; Kangwansupamonkon, W.; Kiatkamjornwong, S. Lignin-based nanogels for the release of payloads in alkaline conditions. *Eur. Polym.*

*J.* **2021**, *145*, No. 110241. (d) Wang, Z.; Li, X.; Zhang, X.; Sheng, R.; Lin, Q.; Song, W.; Hao, L. Novel contact lenses embedded with drug-loaded Zwitterionic nanogels for extended ophthalmic drug delivery. *Nanomaterials* **2021**, *11* (9), No. 2328. (e) Moghadam, F. A. M.; Khoshkalampour, A.; Moghadam, F. A. M.; PourvatanDoust, S.; Naeijian, F.; Ghorbani, M. Preparation and physicochemical evaluation of casein/basil seed gum film integrated with guar gum/gelatin based nanogel containing lemon peel essential oil for active food packaging application. *Int. J. Biol. Macromol.* **2023**, *224*, 786−796.

(12) (a) Win, Y. Y.; Charoenkanburkang, P.; Limprasutr, V.; Rodsiri, R.; Pan, Y.; Buranasudja, V.; Luckanagul, J. A. *In vivo* biocompatible self-assembled nanogel based on hyaluronic acid for aqueous solubility and stability enhancement of asiatic acid. *Polymers* **2021**, *13* (23), No. 4071. (b) Laha, B.; Das, S.; Maiti, S.; Sen, K. K. Novel propyl karaya gum nanogels for bosentan: *in vitro* and *in vivo* drug delivery performance. *Colloids Surf., B* **2019**, *180*, 263−272. (c) Minhas, M. U.; Khan, K. U.; Sarfraz, M.; Badshah, S. F.; Munir, A.; Barkat, K.; Basit, A.; Arafat, M. Polyvinylpyrrolidone K-30-Based Crosslinked Fast Swelling Nanogels: An Impeccable Approach for Drug's Solubility Improvement. *BioMed Res. Int.* **2022**, *2022*, No. 5883239. (d) Cirri, M.; Nerli, G.; Mennini, N.; Maestrelli, F.; Mura, P. Development and Characterization of Cyclodextrin-Based Nanogels as a New Ibuprofen Cutaneous Delivery System. *Pharmaceutics* **2022**, *14* (12), No. 2567.

(13) Organization, W. H.. Leading Causes of Death Globally. https://www.who.int/news-room/fact-sheets/detail/the-top-10-causes-of-death.

(14) Ahmad, F. B.; Cisewski, J. A.; Xu, J.; Anderson, R. N. Provisional mortality data—United States, 2022. *Morb. Mortal. Wkly. Rep.* **2023**, *72* (18), 488−492.

(15) Teng, R.; Maya, J. Absolute bioavailability and regional absorption of ticagrelor in healthy volunteers. *J. Drug Assess.* **2014**, *3* (1), 43−50.

(16) Huang, B.; Qian, Y.; Xie, S.; Ye, X.; Chen, H.; Chen, Z.; Zhang, L.; Xu, J.; Hu, H.; Ma, S.; et al. Ticagrelor inhibits the NLRP3 inflammasome to protect against inflammatory disease independent of the P2Y12 signaling pathway. *Cell. Mol. Immunol.* **2021**, *18* (5), 1278−1289.

(17) Sugidachi, A.; Ohno, K.; Ogawa, T.; Jakubowski, J.; Hashimoto, M.; Tomizawa, A. A comparison of the pharmacological profiles of prasugrel and ticagrelor assessed by platelet aggregation, thrombus formation and haemostasis in rats. *Br. J. Pharmacol.* **2013**, *169* (1), 82−89.

(18) Veitch, A. M.; Vanbiervliet, G.; Gershlick, A. H.; Boustiere, C.; Baglin, T. P.; Smith, L.-A.; Radaelli, F.; Knight, E.; Gralnek, I. M.; Hassan, C.; Dumonceau, J. M. Endoscopy in patients on antiplatelet or anticoagulant therapy, including direct oral anticoagulants: British Society of Gastroenterology (BSG) and European Society of Gastrointestinal Endoscopy (ESGE) guidelines. *Endoscopy* **2016**, *48* (04), 385−402.

(19) Srivastava, A.; Khan, M. A.; Bedi, S.; Bhandari, U. A Review on Different Solubility Enhancement Techniques of Ticagrelor. *Int. J. Pharm. Invest.* **2023**, *13* (1), 1−6.

(20) (a) Tabassum, M.; Pervaiz, F.; Shoukat, H. Fabrication and evaluation of gelatin-PVA-co-poly (2-acrylamido-2-methylpropane sulfonic acid)-based hydrogels for extended-release of sitagliptin and metformin by employing response surface methodology. *Chem. Pap.* **2022**, *76* (7), 4081−4097. (b) Minhas, M. U.; Ahmad, M.; Ali, L.; Sohail, M. Synthesis of chemically cross-linked polyvinyl alcohol-co-poly (methacrylic acid) hydrogels by copolymerization; a potential graft-polymeric carrier for oral delivery of 5-fluorouracil. *Daru, J. Pharm. Sci.* **2013**, *21*, No. 44.

(21) Naeem, A.; Yu, C.; Zang, Z.; Zhu, W.; Deng, X.; Guan, Y. Synthesis and Evaluation of Rutin−Hydroxypropyl $\beta$-Cyclodextrin Inclusion Complexes Embedded in Xanthan Gum-Based (HPMC-g-AMPS) Hydrogels for Oral Controlled Drug Delivery. *Antioxidants* **2023**, *12* (3), No. 552.

(22) (a) Na, Y.-G.; Byeon, J.-J.; Wang, M.; Huh, H. W.; Son, G.-H.; Jeon, S.-H.; Bang, K.-H.; Kim, S.-J.; Lee, H.-J.; Lee, H.-K. Strategic approach to developing a self-microemulsifying drug delivery system to enhance antiplatelet activity and bioavailability of ticagrelor. *Int. J. Nanomed.* **2019**, 1193−1212. (b) Son, G.-H.; Na, Y.-G.; Huh, H. W.; Wang, M.; Kim, M.-K.; Han, M.-G.; Byeon, J.-J.; Lee, H.-K.; Cho, C.-W. Systemic design and evaluation of ticagrelor-loaded nano-structured lipid carriers for enhancing bioavailability and antiplatelet activity. *Pharmaceutics* **2019**, *11* (5), No. 222. (c) Na, Y.-G.; Pham, T. M. A.; Byeon, J.-J.; Kim, M.-K.; Han, M.-G.; Baek, J.-S.; Lee, H.-K.; Cho, C.-W. Development and evaluation of TPGS/PVA-based nanosuspension for enhancing dissolution and oral bioavailability of ticagrelor. *Int. J. Pharm.* **2020**, *581*, No. 119287. (d) Kim, S.-J.; Lee, H.-K.; Na, Y.-G.; Bang, K.-H.; Lee, H.-J.; Wang, M.; Huh, H.-W.; Cho, C.-W. A novel composition of ticagrelor by solid dispersion technique for increasing solubility and intestinal permeability. *Int. J. Pharm.* **2019**, *555*, 11−18.

(23) Tanveer, S.; Ahmad, M.; Minhas, M. U.; Ahmad, A.; Khan, K. U. Chitosan-PVA-co-poly (2-acrylamido-2-methylpropane sulfonic acid) cross-linked hybrid IPN-nanogels for transdermal delivery of ondansetron; synthesis, characterization and toxicological evaluation. *Polym.-Plast. Technol. Mater.* **2021**, *60* (17), 1913−1934.

(24) Guaresti, O.; Maiz−Fernández, S.; Palomares, T.; Alonso−Varona, A.; Eceiza, A.; Pérez−Álvarez, L.; Gabilondo, N. Dual charged folate labelled chitosan nanogels with enhanced mucoadhesion capacity for targeted drug delivery. *Eur. Polym. J.* **2020**, *134*, No. 109847.

(25) Rao, K. M.; Mallikarjuna, B.; Rao, K. K.; Siraj, S.; Rao, K. C.; Subha, M. Novel thermo/pH sensitive nanogels composed from poly (N-vinylcaprolactam) for controlled release of an anticancer drug. *Colloids Surf., B* **2013**, *102*, 891−897.

(26) Fan, B.; Xing, Y.; Zheng, Y.; Sun, C.; Liang, G. pH-responsive thiolated chitosan nanoparticles for oral low-molecular weight heparin delivery: *in vitro* and *in vivo* evaluation. *Drug Delivery* **2016**, *23* (1), 238−247.

(27) Sarika, P.; Kumar, P. A.; Raj, D. K.; James, N. R. Nanogels based on alginic aldehyde and gelatin by inverse miniemulsion technique: synthesis and characterization. *Carbohydr. Polym.* **2015**, *119*, 118−125.

(28) Ashames, A.; Ullah, K.; Al-Tabakha, M.; Khan, S. A.; Hassan, N.; Mannan, A.; Ikram, M.; Buabeid, M.; Murtaza, G. Development, characterization and In-vitro evaluation of guar gum based new polymeric matrices for controlled delivery using metformin HCl as model drug. *PLoS One* **2022**, *17* (7), No. e0271623.

(29) Alam, A.; Jawaid, T.; Alsanad, S. M.; Kamal, M.; Rawat, P.; Singh, V.; Alam, P.; Alam, P. Solubility Enhancement, Formulation Development, and Antibacterial Activity of Xanthan-Gum-Stabilized Colloidal Gold Nanogel of Hesperidin against Proteus Vulgaris. *Gels* **2022**, *8* (10), No. 655.

(30) Aminu, N.; Chan, S.-Y.; Yam, M.-F.; Toh, S.-M. A dual-action chitosan-based nanogel system of triclosan and flurbiprofen for localised treatment of periodontitis. *Int. J. Pharm.* **2019**, *570*, No. 118659.

(31) Zhang, Y.; Huo, M.; Zhou, J.; Zou, A.; Li, W.; Yao, C.; Xie, S. DDSolver: an add-in program for modeling and comparison of drug dissolution profiles. *AAPS J.* **2010**, *12*, 263−271.

(32) Abbas, G.; Rasul, A.; Fakhar-e-Alam, M.; Saadullah, M.; Muzammil, S.; Iqbal, O.; Atif, M.; Hanif, M.; Shah, S.; Ahmad, S.; et al. Nanoparticles of thiolated chitosan for controlled delivery of moxifloxacin: In-vitro and in-vivo evaluation. *J. King Saud Univ., Sci.* **2022**, *34* (7), No. 102218.

(33) Ren, X.; Qi, J.; Wu, W.; Yin, Z.; Li, T.; Lu, Y. Development of carrier-free nanocrystals of poorly water-soluble drugs by exploring metastable zone of nucleation. *Acta Pharm. Sin. B* **2019**, *9* (1), 118−127.

(34) Cacua, K.; Ordoñez, F.; Zapata, C.; Herrera, B.; Pabón, E.; Buitrago-Sierra, R. Surfactant concentration and pH effects on the zeta potential values of alumina nanofluids to inspect stability. *Colloids Surf., A* **2019**, *583*, No. 123960.



https://doi.org/10.1021/acsomega.4c01721
*ACS Omega* 2024, 9, 21401−21415

(35) Sultana, H.; Aamir, M. N.; Madni, A.; ur Rehman, M.; Shafiq, A.; Shirazi, J. H.; Hassan, S.; Sumaira. Polymeric Nanogel for Oral Delivery of the Chemotherapeutic Agent: Fabrication and Evaluation Alongside Toxicological Studies and Histopathological Examination. *AAPS PharmSciTech* **2023**, *24* (1), No. 43.
(36) Shahid, N.; Erum, A.; Zaman, M.; Iqbal, M. O.; Riaz, R.; Tulain, R.; Hussain, T.; Amjad, M. W.; Raja, M. A.; Farooq, U.; Aman, W. Fabrication of thiolated chitosan based biodegradable nanoparticles of ticagrelor and their pharmacokinetics. *Polym. Polym. Compos.* **2022**, *30*, No. 09673911221108742.
(37) Betti, N. A. Thermogravimetric analysis on PVA/PVP blend under air atmosphere. *Eng. Technol. J.* **2016**, *34* (13A), 2433−2442.
(38) Anwar, H.; Ahmad, M.; Minhas, M. U.; Rehmani, S. Alginate-polyvinyl alcohol based interpenetrating polymer network for prolonged drug therapy, optimization and in-vitro characterization. *Carbohydr. Polym.* **2017**, *166*, 183−194.
(39) (a) Shoukat, H.; Pervaiz, F.; Noreen, S.; Nawaz, M.; Qaiser, R.; Anwar, M. Fabrication and evaluation studies of novel polyvinylpyrrolidone and 2-acrylamido-2-methylpropane sulphonic acid-based crosslinked matrices for controlled release of acyclovir. *Polym. Bull.* **2020**, *77*, 1869−1891. (b) Ashames, A.; Pervaiz, F.; Al-Tabakha, M.; Khalid, K.; Hassan, N.; Shoukat, H.; Buabeid, M.; Murtaza, G. Synthesis of cross-linked carboxymethyl cellulose and poly (2-acrylamido-2-methylpropane sulfonic acid) hydrogel for sustained drug release optimized by Box-Behnken Design. *J. Saudi Chem. Soc.* **2022**, *26* (6), No. 101541.
(40) Shahid, N.; Erum, A.; Zaman, M.; Tulain, U. R.; Shoaib, Q.-U.-A.; Majeed, A.; Rasool, M. F.; Imran, I.; Alshehri, S.; Noorani, B.; Alqahtani, F. pH-Responsive nanocomposite based hydrogels for the controlled delivery of ticagrelor; *in vitro* and *in vivo* approaches. *Int. J. Nanomed.* **2021**, *16*, 6345−6366.
(41) (a) Taleb, M. A.; Hegazy, D. E.; Mahmoud, G. A. Characterization and *in vitro* drug release behavior of (2-hydroxyethyl methacrylate)−co-(2-acrylamido-2-methyl-1-propanesulfonic acid) crosslinked hydrogels prepared by ionizing radiation. *Int. J. Polym. Mater. Polym. Biomater.* **2014**, *63* (16), 840−845. (b) Devi, N.; Narzary, A. Release dynamics of brufen from a drug-loaded polymer hydrogel containing polyvinyl alcohol, 2-acrylamide-2-methylpropane sulfonic acid and acrylamide. *Int. J. Polym. Mater.* **2012**, *61* (11), 821−833.
(42) Abdullah, O.; Minhas, M. U.; Ahmad, M.; Ahmad, S.; Barkat, K.; Ahmad, A. Synthesis, optimization, and evaluation of polyvinyl alcohol-based hydrogels as controlled combinatorial drug delivery system for colon cancer. *Adv. Polym. Technol.* **2018**, *37* (8), 3348−3363.
(43) Durmaz, S.; Okay, O. Acrylamide/2-acrylamido-2-methylpropane sulfonic acid sodium salt-based hydrogels: synthesis and characterization. *Polymer* **2000**, *41* (10), 3693−3704.
(44) Hassan, S. U.; Khalid, I.; Hussain, L.; Barkat, K.; Khan, I. U. Development and evaluation of pH-responsive pluronic f 127 Co-poly-(Acrylic acid) biodegradable nanogels for topical delivery of terbinafine HCL. *Dose-Response* **2022**, *20* (2), No. 15593258221095977.
(45) Sarfraz, R. M.; Khan, M. U.; Mahmood, A.; Akram, M. R.; Minhas, M. U.; Qaisar, M. N.; Ali, M. R.; Ahmad, H.; Zaman, M. Synthesis of co-polymeric network of Carbopol-g-methacrylic acid nanogels drug carrier system for gastro-protective delivery of ketoprofen and its evaluation. *Polym.-Plast. Technol. Mater.* **2020**, *59* (10), 1109−1123.
(46) (a) Shoukat, H.; Pervaiz, F.; Khan, M.; Rehman, S.; Akram, F.; Abid, U.; Noreen, S.; Nadeem, M.; Qaiser, R.; Ahmad, R.; Farooq, I. Development of $\beta$-cyclodextrin/polyvinypyrrolidone-co-poly (2-acrylamide-2-methylpropane sulphonic acid) hybrid nanogels as nano-drug delivery carriers to enhance the solubility of Rosuvastatin: An *in vitro* and *in vivo* evaluation. *PLoS One* **2022**, *17* (1), No. e0263026. (b) Ahmad, W.; Khalid, I.; Barkat, K.; Minhas, M. U.; Khan, I. U.; Syed, H. K.; Mali, N. S.; Jamshed, A.; Ikram, A.; Badshah, M. Development and evaluation of polymeric nanogels to enhance solubility of letrozole. *Polym. Bull.* **2023**, *80* (4), 4085−4116.
(47) Gao, Y.; Zuo, J.; Bou-Chacra, N.; de Jesus Andreoli Pinto, T.; Clas, S.-D.; Walker, R. B.; Löbenberg, R. *In vitro* release kinetics of antituberculosis drugs from nanoparticles assessed using a modified dissolution apparatus. *BioMed Res. Int.* **2013**, *2013*, No. 136590.
(48) Iqbal, O.; Shah, S.; Abbas, G.; Rasul, A.; Hanif, M.; Ashfaq, M.; Afzal, Z. Moxifloxacin loaded nanoparticles of disulfide bridged thiolated chitosan-eudragit RS100 for controlled drug delivery. *Int. J. Biol. Macromol.* **2021**, *182*, 2087−2096.
(49) Khalid, Q.; Ahmad, M.; Minhas, M. U.; Batool, F.; Malik, N. S.; Rehman, M. Novel $\beta$-cyclodextrin nanosponges by chain growth condensation for solubility enhancement of dexibuprofen: Characterization and acute oral toxicity studies. *J. Drug Delivery Sci. Technol.* **2021**, *61*, No. 102089.


https://doi.org/10.1021/acsomega.4c01721
*ACS Omega* 2024, 9, 21401−21415